Stem Cell Reports
Article

OPEN ACCESS

Hematopoietic Stem Cells but Not Multipotent Progenitors Drive Erythropoiesis during Chronic Erythroid Stress in EPO Transgenic Mice

Rashim Pal Singh,[1,7] Tatyana Grinenko,[1,7] Beáta Ramasz,[1] Kristin Franke,[1] Mathias Lesche,[2] Andreas Dahl,[2] Max Gassmann,[3,6] Triantafyllos Chavakis,[1,4] Ian Henry,[5] and Ben Wielockx[1,4,*]

[1]Institute for Clinical Chemistry and Laboratory Medicine, Technische Universität Dresden, Fetscherstraße 74, Dresden 01307, Germany
[2]Deep Sequencing Group SFB 655, Biotechnology Center; Technische Universität Dresden, Fetscherstraße 105, Dresden 01307, Germany
[3]Institute of Veterinary Physiology, Vetsuisse Faculty and Zurich Center for Integrative Human Physiology (ZIHP), University of Zürich, Winterthurerstr. 190, Zürich 8057, Switzerland
[4]DFG Research Center and Cluster of Excellence for Regenerative Therapies Dresden, Technische Universität Dresden, Fetscherstraße 105, Dresden 01307, Germany
[5]Max Planck Institute of Molecular Cell Biology and Genetics, Pfotenhauerstraße 108, Dresden 01307, Germany
[6]Universidad Peruana Cayetano Heredia (UPCH), Av. Honorio Delgado 430, San Martín de Porres 15102, Peru
[7]Co-first author
*Correspondence: ben.wielockx@tu-dresden.de
https://doi.org/10.1016/j.stemcr.2018.04.012

SUMMARY

The hematopoietic stem cell (HSC) compartment consists of a small pool of cells capable of replenishing all blood cells. Although it is established that the hematopoietic system is assembled as a hierarchical organization under steady-state conditions, emerging evidence suggests that distinct differentiation pathways may exist in response to acute stress. However, it remains unclear how different hematopoietic stem and progenitor cell subpopulations behave under sustained chronic stress. Here, by using adult transgenic mice overexpressing erythropoietin (EPO; Tg6) and a combination of *in vivo*, *in vitro*, and deep-sequencing approaches, we found that HSCs respond differentially to chronic erythroid stress compared with their closely related multipotent progenitors (MPPs). Specifically, HSCs exhibit a vastly committed erythroid progenitor profile with enhanced cell division, while MPPs display erythroid and myeloid cell signatures and an accumulation of uncommitted cells. Thus, our results identify HSCs as master regulators of chronic stress erythropoiesis, potentially circumventing the hierarchical differentiation-detour.

INTRODUCTION

All lineages of hematopoietic cells, including those of the erythroid lineage, arise from a unique population of hematopoietic stem cells (HSCs) (Clapes et al., 2016). However, whether all mature blood cells are derived from these HSCs or from downstream multipotent progenitors (MPPs) during steady-state hematopoiesis remains contentious (Busch et al., 2015; Sawai et al., 2016; Sun et al., 2014). Previous work in the field of HSC biology has mainly focused on acute stress, including bone marrow (BM) injury or infection (Haas et al., 2015), which typically triggers an increase of HSCs that enter the cell cycle; HSCs return to quiescence when homeostasis is re-established (Baldridge et al., 2010; Trumpp et al., 2010). Interestingly, a number of studies have also suggested that HSCs and MPPs can circumvent these distinct intermediate stages (Haas et al., 2015; Pietras et al., 2015; Sanjuan-Pla et al., 2013; Yamamoto et al., 2013).

Recently, attention is being drawn to the chronic effects of emergency signals (such as interleukin-1 [IL-1]), their impact on the immune system, and their long-term consequences on the HSC compartment (Pietras et al., 2016). However, much remains to be understood regarding how chronic overexpression of lineage-specific proteins such as erythropoietin (EPO) may influence HSC/MPP fate. The latter hormone is the principal stimulator of erythropoiesis, a complex multistep process during which erythroid progenitors develop into mature red blood cells (RBCs). EPO binding to its receptor (EPO-R) activates multiple pathways, including the JAK/STAT and the MAPK-ERK1/2 pathways, which reduce apoptosis and promote expansion and differentiation of erythroid progenitors (Dunlop et al., 2006; Franke et al., 2013a; Gassmann and Muckenthaler, 2015). Increased EPO production resulting from mutations in specific members of the hypoxia-inducible factor (HIF) pathway (e.g., VHL, HIF2α, or PHD2) may lead to secondary erythrocytosis, representing the aberrant increase in RBC numbers (Franke et al., 2013b). In this report, using the well-defined EPO transgenic mouse line (Tg6) (Ruschitzka et al., 2000), we establish that HSCs and MPPs respond differently to chronic and sustained erythroid stress. Specifically, HSCs display a substantial erythroid progenitor profile in a quest to differentiate into erythrocytes potentially bypassing numerous downstream progenitors, while MPPs limit their internal commitment toward myeloid progenitors.

RESULTS

To understand the role of chronic and sustained erythroid stress on the entire hematopoietic compartment, we used

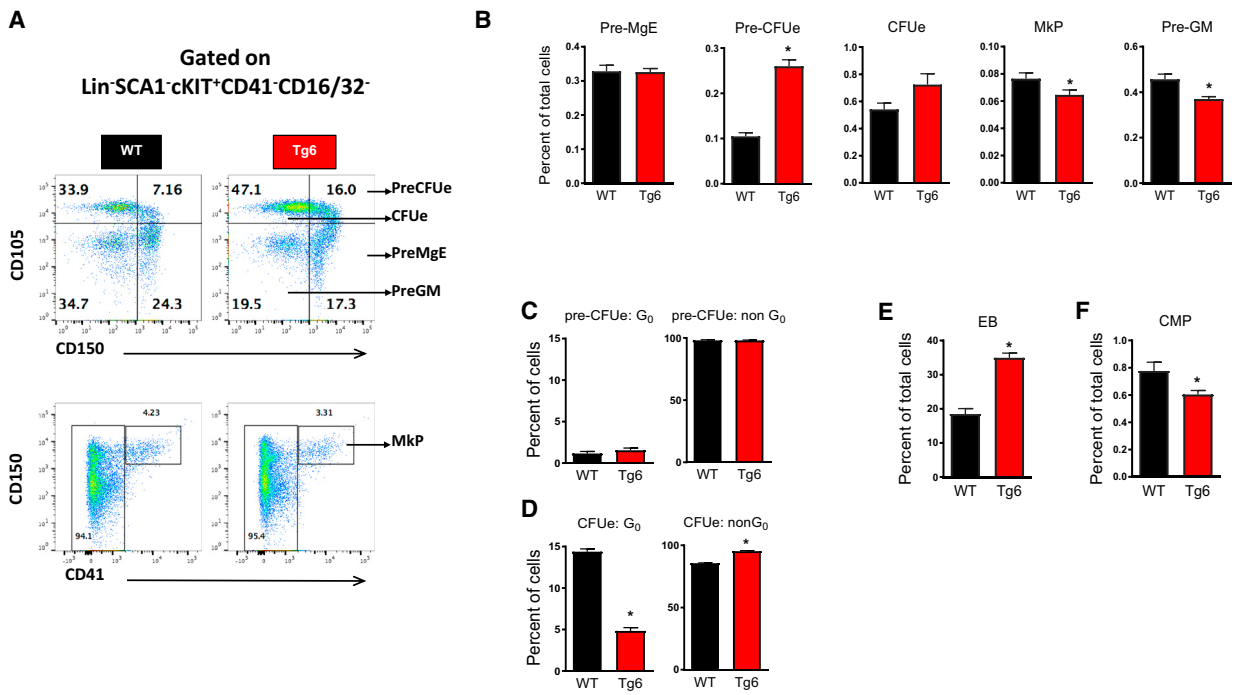

Figure 1. Sustained Chronic Exposure to High Systemic EPO Levels Leads to Dramatic Changes in Myeloid/Erythroid Progenitor

(A) Gating strategy for the myeloid-erythroid-megakaryocyte progenitors gated on Lin$^-$ SCA-1$^-$ cKIT$^+$ CD41$^-$ CD16/32$^-$ according to Pronk et al. (2007).

(B) Bar graphs showing Pre-MgE (Lin$^-$ SCA-1$^-$ cKIT$^+$ CD41$^-$ CD16/32$^-$ CD105$^-$ CD150$^+$), Pre-CFUe (Lin$^-$SCA-1$^-$ cKIT$^+$ CD41$^-$ CD16/32$^-$ CD105$^+$ CD150$^+$), CFUe (Lin$^-$ SCA-1$^-$ cKIT$^+$ CD41$^-$ CD16/32$^-$ CD105$^+$ CD150$^-$), MkP (Lin$^-$ SCA-1$^-$ cKIT$^+$ CD41$^+$ CD16/32$^-$ CD150$^+$), and Pre-GM (Lin$^-$ SCA-1$^-$ cKIT$^+$ CD41$^-$ CD16/32$^-$ CD105$^-$ CD150$^-$) (n = 5–6), and one of three representative experiments is shown.

(C and D) Cell-cycle analysis of Pre-CFUe (C) and CFUe cells from WT and Tg6 mice (D). Bar graphs representing the fraction of progenitors in the quiescent G0 phase of the cell cycle (left) and progressing through the cell cycle (non-G0, right) (n = 4). Gating strategy for cell-cycle analysis of cells is as shown in Figure S2A for HSC and MPP.

(E and F) EB (CD71$^+$ Ter119$^+$) (n = 4) (E) and CMP (Lin$^-$ SCA-1$^-$ cKIT$^+$ CD34$^+$ CD16/32$^-$) (n = 5–6) (F).

(C–F) Data are representative for two to three independent experiments. n denotes individual mice. Values are mean ± SEM. *p < 0.05. See also Figure S1.

the well-defined EPO transgenic mouse line (Tg6). Independent of the oxygen conditions, these mice constitutively show high serum levels of human EPO, resulting in excessive production of RBCs (Figure S1A) (Ruschitzka et al., 2000). The bipotent pre-megakaryocyte erythrocyte progenitor (Pre-MgE), which is upstream of the more committed erythroid-restricted progenitor (Pre-CFUe), the CFUe (colony-forming unit erythroid) and erythroblasts (EBs), have been suggested as the first cells in the hematopoietic tree to robustly express EPO-R during hematopoiesis in humans (Seita et al., 2012). Although Tg6 mice did not display any alteration in Pre-MgE as compared with wild-type (WT) mice, the relative proportions of Pre-CFUe, but not CFUe, were significantly higher in Tg6 mice. Conversely, megakaryocyte progenitors (MkP) and pre-granulocyte-monocyte lineage cells (Pre-GM) were significantly reduced (Figures 1A, 1B, and S1B; gating according to Pronk et al., 2007). Furthermore, compared with Pre-CFUe, Tg6 CFUe's were progressing significantly more through the cell cycle compared with WT CFUe's (Figures 1C and 1D), strongly indicating a prominent proliferation/differentiation impulse toward downstream EBs (Figures 1E and S1C; gating according to Dumitriu et al., 2010) and RBCs (Figure S1A). Upstream of Pre-GM, common myeloid progenitors (CMPs) were also reduced in Tg6 BM cells (Figures 1F and S1D; gating according to Akashi et al., 2000). We next analyzed the HSC/MPP compartment immediately upstream of the CMPs, which consists of a heterogeneous population. Interestingly, although the HSC fraction (CD48$^-$/CD150$^+$ Lineage$^-$ SCA-1$^+$ Kit$^+$ [LSK] (= LT-HSC and MPP1 [Wilson et al., 2008]) displayed a significant increase in absolute numbers but not in its relative abundance, the MPP population (CD48$^+$/CD150$^-$ LSK cells (= MPP3 and MPP4 [Wilson et al., 2008]) was both relatively and absolutely expanded more than 2-fold, compared with WT littermates (Figures 2A and

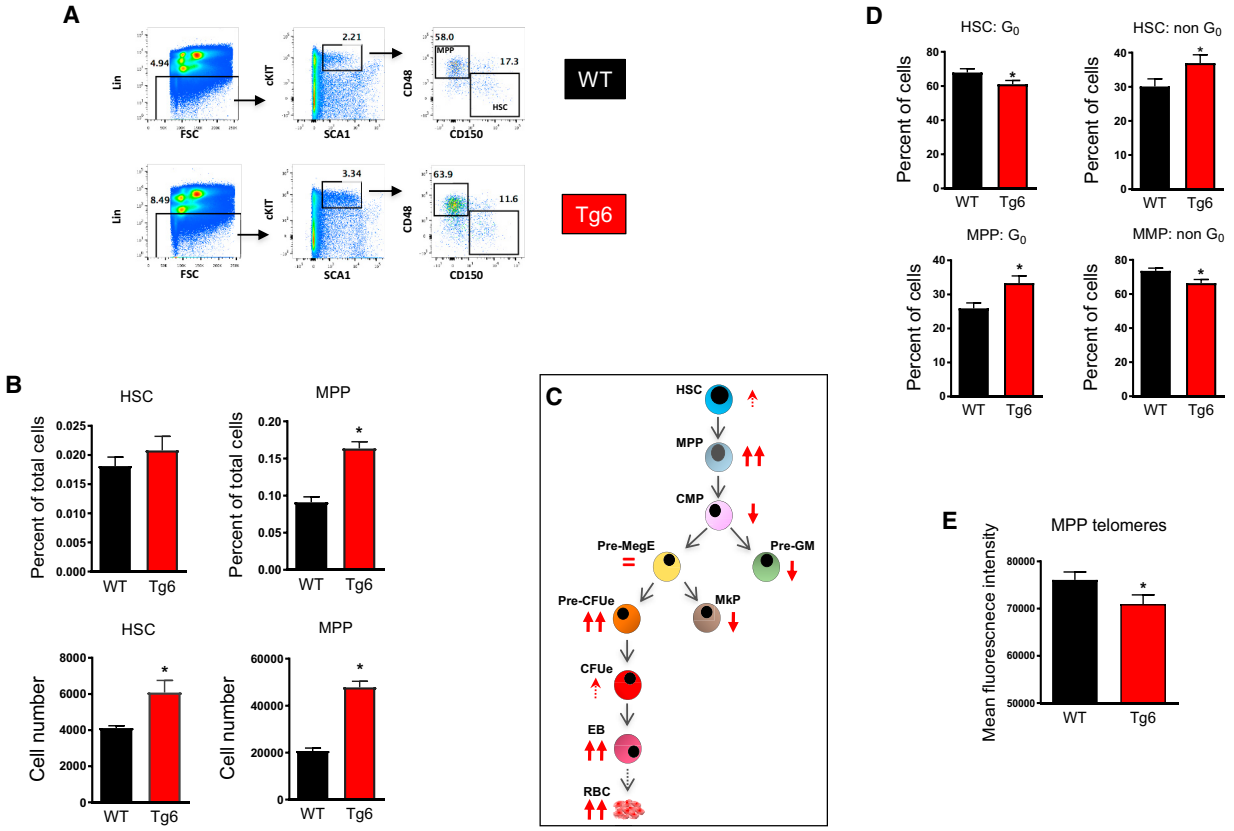

Figure 2. Tg6 Mice Display an Increased HSC/MPP Compartment

(A) Gating strategy and representative fluorescence-activated cell sorting (FACS) plots of hematopoietic stem progenitor cell populations.

(B) Proportion and total HSC and MPP numbers from WT and Tg6 mice (n = 5–7), one of more than five representative experiments is shown.

(C) The overall effect of chronic and continuous high EPO exposure on the classical representation of the hematopoietic tree taken from data presented in Figures 1, 2, and S1.

(D) Bar graphs representing the fraction of HSCs and MPPs in the quiescent G0 phase of the cell cycle (left) and progressing through the cell cycle (non-G0, right), (n = 15–17), from four independent experiments. Gating strategy as shown in Figure S2A.

(E) Relative telomere length of isolated MPPs from both genotypes (n = 5–6). Values are mean ± SEM. *p < 0.05.

See also Figure S2.

2B). Together, these observations suggest a long-term surge in erythroid progenitor populations at the expense of myeloid progenitors, starting with CMP (Figure 2C).

To understand this differential response between HSCs and MPPs, and the reduction in downstream myeloid progenitors, we studied cell-cycle progression in the hematopoietic stem and progenitor cell (HSPC) compartment. To this end, we found that a significantly higher number of Tg6 HSCs progressed through the cell cycle compared with WT HSCs. In contrast, Tg6 MPPs were more quiescent compared with their WT counterparts (Figures S2A and 2D). As the latter displays an apparent discrepancy with the increase in total MPP numbers, we decided to define the telomere lengths in MPPs from Tg6 and WT mice, as these are a measure of the number of times a (stem) cell has divided over time (Chiu et al., 1996). Our analyses revealed significantly shorter telomeres in Tg6 MPPs than in WT MPPs, which suggests longer overall survival and subdued differentiation (less downstream progenitors) of Tg6 MPPs, despite reduced instant proliferation. Furthermore, we also examined MPPs in 4-week-old mice and found a clear trend toward lower numbers of Tg6 MPPs compared with WT littermates (Figure S2B). Conversely, we found no increased cycling of Tg6 MPPs in these 4-week-old mice (Figure S2C), although MPP cell numbers in 6-week-old animals were no longer different (Figure S2B) and further reverted in adult mice (Figure 2B). This further supports the notion that, already at an early stage, Tg6 MPPs show more preference to self-renew than to differentiate in comparison with WT MPPs.

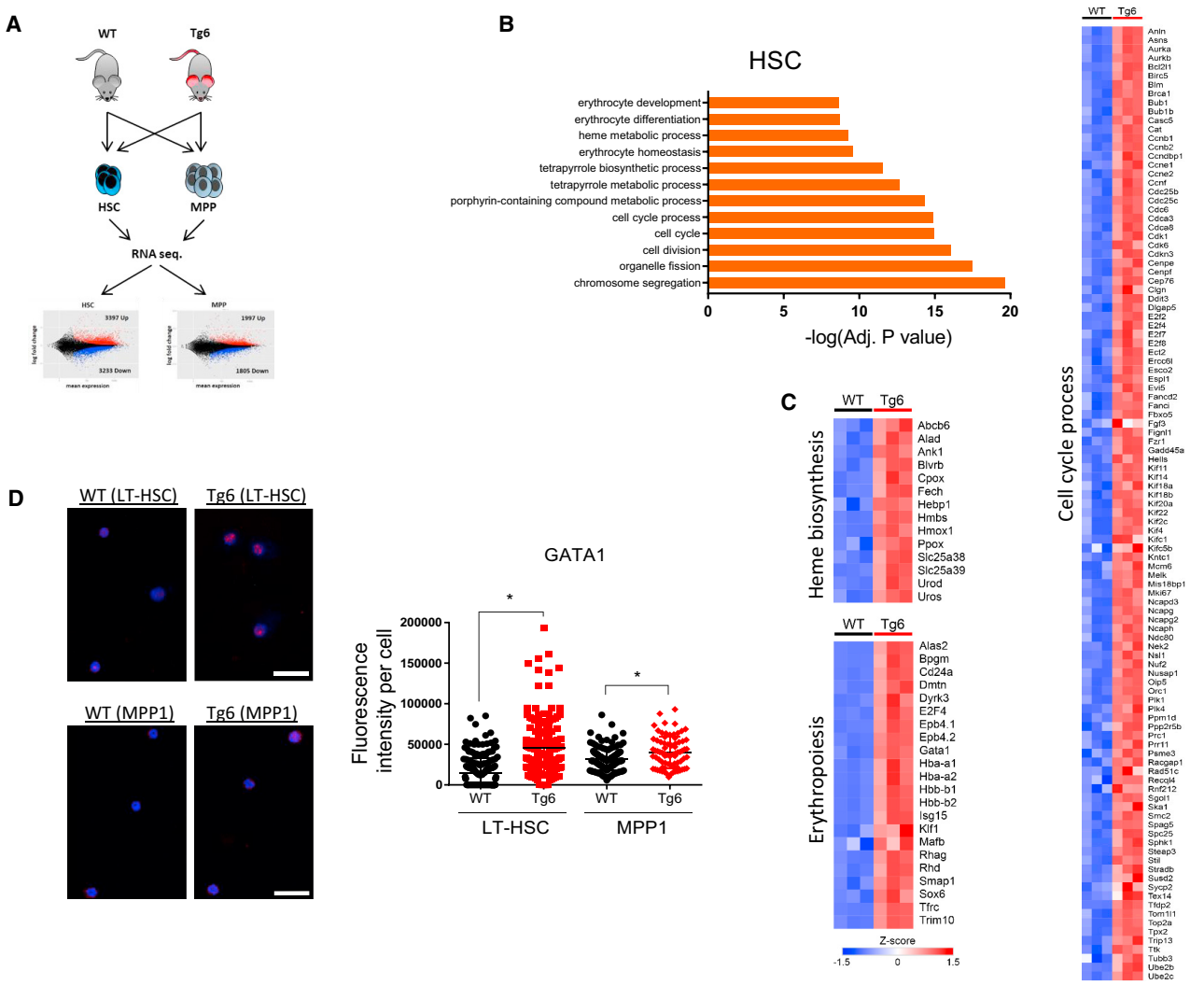

Figure 3. Sustained and Chronic High EPO Induces Erythroid Transcriptional Reprograming in HSCs

(A) Schematic overview of the transcriptome sequencing setup to compare HSCs/MPPs from Tg6 and WT littermates (three samples per genotype, and each sample contained cells from three individual mice).

(B) Adapted networks of the highest represented GO terms of genes with ≥2-fold overexpression in Tg6 HSCs versus WT littermate HSCs.

(C) Heatmaps depicting all genes from the HSC GO terms represented in (B).

(D) Immunofluorescent staining of the GATA1 transcription factor in sorted LT-HSC and MPP1 isolated from adult WT and Tg6 mice. Scale bars represent 25 μm. GATA1 expression in sorted single cells defined by fluorescent intensity per cell. Data are representative for two independent experiments. Representation of GATA1-prefered sites are shown in Figure S3C. Values are mean ± SEM. *p < 0.05.

See also Figures S3 and S4 and Table S1.

To unravel the differential response of HSCs and MPPs to chronic and sustained EPO exposure, we performed a global transcriptome analysis, which uncovered a strong divergence between hematopoietic progenitor populations from Tg6 and WT mice (Figures 3A and S3A). Specifically, HSCs from Tg6 and WT mice revealed more than 6,600 significantly differentially expressed genes (DEGs), while that for MPPs was about 3,800 DEGs (Figures 3A and S3B). Ontology analyses of genes that were at least 2-fold upregulated in the HSCs and MPPs of Tg6 mice (Huang da et al., 2009) indicated that HSCs from Tg6 mice were significantly enriched in genes directly related to RBC production (Figure 3B). These included transcripts involved in erythrocyte structure (*Dmtn, Epb4.1*, and *4.2*), heme biosynthesis (e.g., all eight core members, namely *Alas2, Alad, Cpox, Fech, Hmbs, Uros, Urod,* and *Ppox* [Nilsson et al., 2009]), as well as a set of transcription factors directly related to erythropoiesis, including *Gata1, E2F4, Klf1*, and

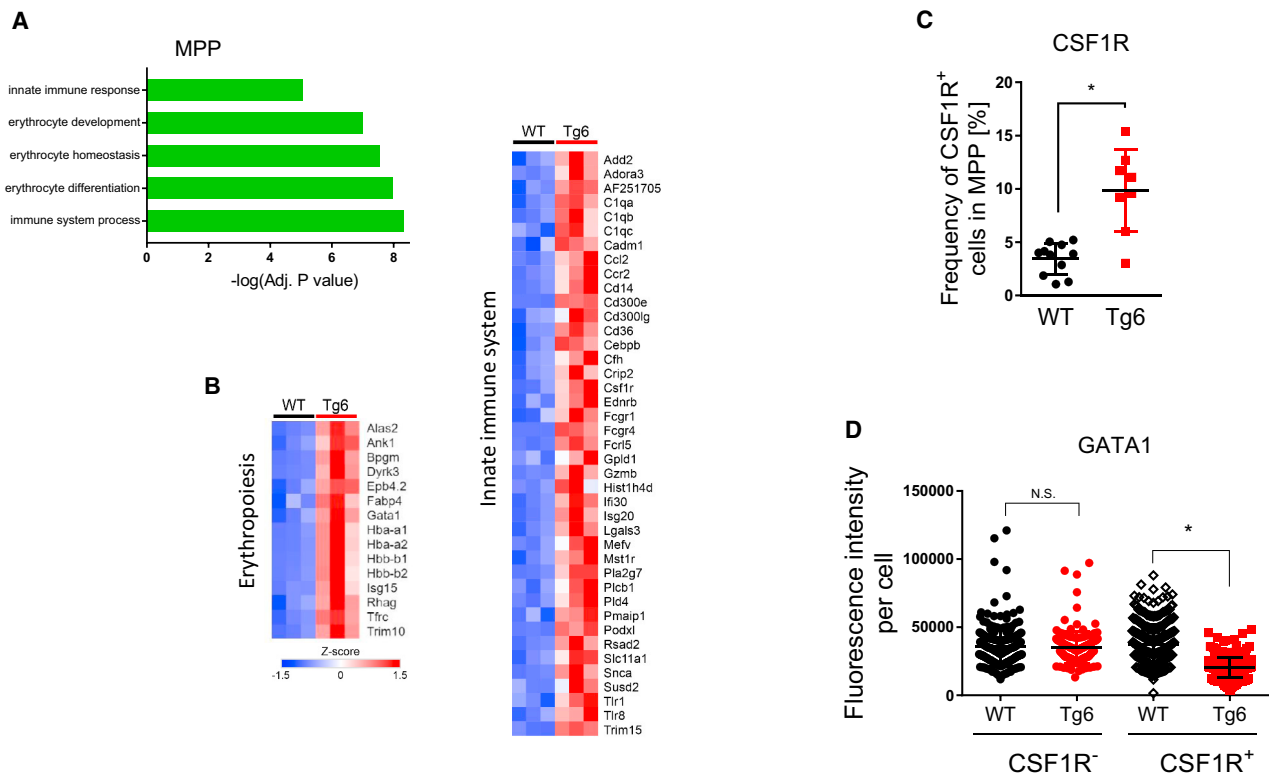

Figure 4. Sustained and Chronic High EPO Induces a Dual Signature in MPPs

(A) Adapted networks of the highest represented GO terms of genes with ≥2-fold overexpression in Tg6 MPPs versus WT littermate MPPs.

(B) Heatmaps depicting all genes from the MPP GO terms represented in (A).

(C) Proportion of CSF1R$^+$ cells in Tg6 versus WT MPPs.

(D) GATA1 expression in sorted single cells defined by fluorescent intensity per cell.

Data in (C) and (D) are representative for two independent experiments. Values are mean ± SEM. *$p < 0.05$.

See also Figure S4 and Table S2.

Sox6 (Figures 3B and 3C) (Dumitriu et al., 2010; Gutierrez et al., 2008; Humbert et al., 2000; Shah et al., 2015). Parallel to these findings and our initial observations in Tg6 HSCs, numerous gene ontology (GO) terms related to the "cell-cycle process" were uncovered, which corresponded to more than 100 Tg6 HSCs genes (≥2-fold) significantly overexpressed in the diverse phases of the division process (Figures 3B and 3C).

To support these results, we performed immunofluorescent staining for GATA1 on sorted cells. We stained LT-HSC and MPP1 separately (CD34$^-$ and CD34$^+$ HSCs, respectively) as it was shown previously that the latter population can give rise to stress erythroid progenitors (Harandi et al., 2010). Interestingly, both Tg6 fractions showed a significant increase in GATA1 staining compared with their respective WT control cells (Figure 3D). Further, we found an increase in all target genes with "GATA1-prefered sites" that contribute to erythroid differentiation (Figure S3C) (Suzuki et al., 2013), and a significant downregulation of *Gata2* (Figure S3D), an HSC-specific transcription factor that is directly and transcriptionally repressed, and physically replaced from chromatin, by GATA1 (Bresnick et al., 2010).

In stark contrast with RNA sequencing (RNA-seq) data from HSPCs after acute exposure to high EPO (Grover et al., 2014), the Tg6 MPPs displayed GO terms that are positively associated with the innate immune system (Figure 4A). Moreover, a large set of myeloid lineage markers such as *mst1r* (*macrophage-stimulating protein 1 receptor*), *Tlr1* (*Toll-like receptor 1*), *Cebpb (CCAAT/enhancer-binding protein beta*), and *Csf1r (macrophage colony-stimulating factor 1 receptor*) were highly upregulated, with only a less-pronounced link toward erythropoiesis, especially in comparison with the erythroid genes induced in Tg6 HSCs (Figures 4B and S4A). CSF1R is a receptor for the macrophage colony-stimulating factor, and is known to influence HSPC differentiation into monocytes/macrophages (Stanley and Chitu, 2014). Consistently, we also demonstrate that a significantly higher fraction of Tg6 MPPs display CSF1R on their surface (Figure 4C); this is, however,

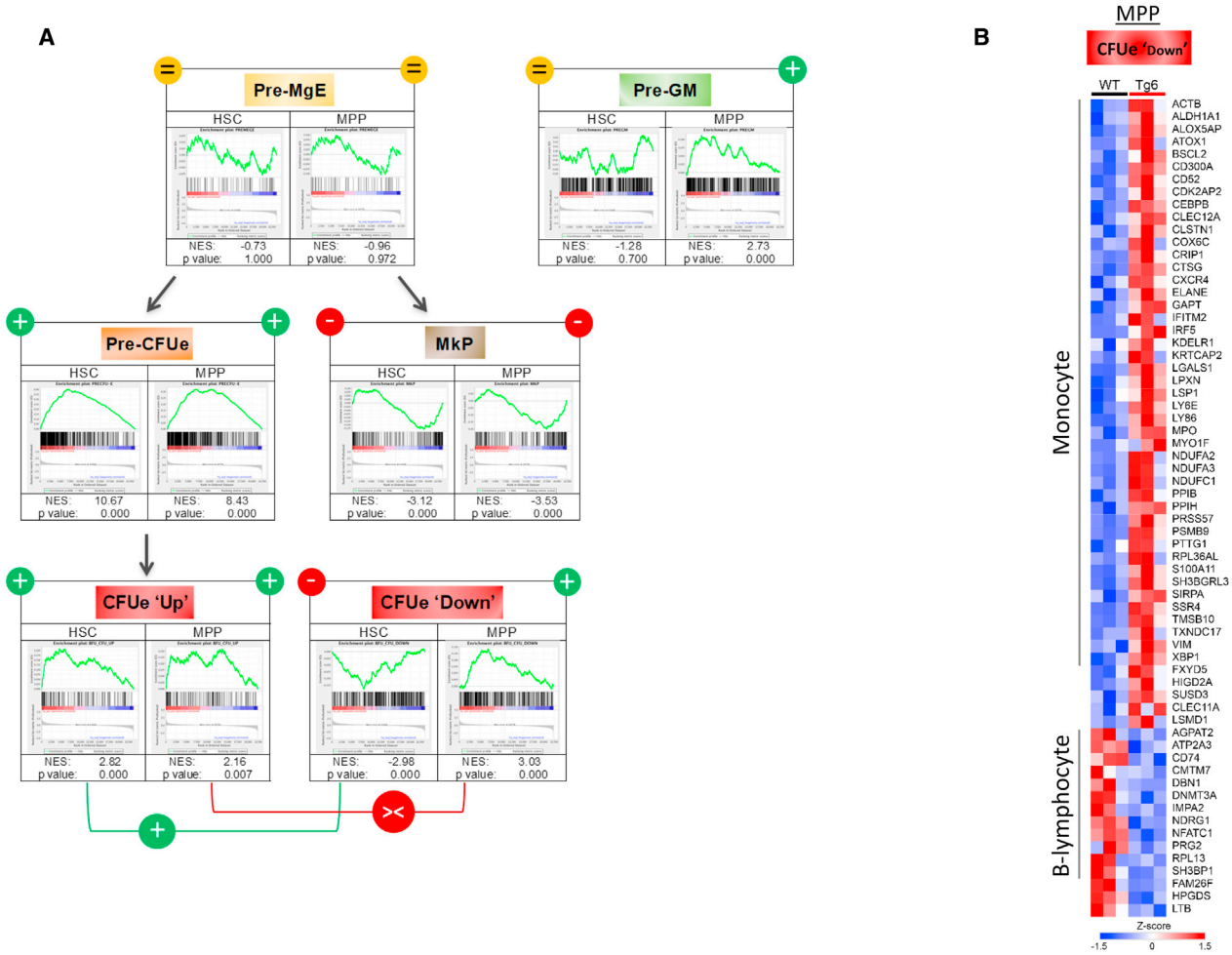

Figure 5. Tg6 HSCs Have a Clear Erythroid Signature, while the MPP Fraction Displays Two Different Signatures

(A) GSEA of significantly upregulated genes from Tg6 HSCs and MPPs compared with sets of genes from different erythroid/myeloid/megakaryocyte progenitors, as shown in Figure 2C. Signs in the upper corner of the tables (+, −, =) designate correlation of the signature with respective progenitor (HSC → left, MPP → right) based on p value. Both signs underneath the CFUe tables reflect the potential subsequent effect of the "up" or "down" signatures (><, opposing). p value as indicated (if p = 0.000, then p < 0.0001).

(B) Heatmap depicting all 65 significantly changed Tg6 MPP genes represented in the CFUe down signature (GSEA).

independent of a potential increase in the myeloid-biased MPP3 cell population, as their relative percentages remained comparable between Tg6 and WT mice (Figure S4B). In addition, we found no difference in GATA1 staining between both genotypes in a majority of their MPPs ($CSF1R^-$), although $CSF1R^+$ Tg6 MPPs contained significantly less GATA1 than their control littermates (Figure 4D).

To better define EPO-induced alterations in HSCs and MPPs, we used published profile data on committed progenitors (Li et al., 2014; Sanjuan-Pla et al., 2013); specifically, we evaluated the gene signatures of various lineages using gene set enrichment analysis (GSEA) (Mootha et al., 2003; Subramanian et al., 2005). GSEA revealed that both stem cells and progenitors from Tg6 mice displayed matching Pre-CFUe signatures, which contrasted with the strong negative signature for the MkP gene set (Figure 5A). Downstream of the Pre-CFUe, HSCs and MPPs exhibited a positive signature for transcripts known to be upregulated in CFUe cells (CFUe Up). Remarkably, the Tg6 MPP fraction also contained a large set of significantly induced genes that, according to CFUe signature, are expected to be downregulated (normalized enrichment scores [NES]: +3.03; CFUe down) (Li et al., 2014), while Tg6 HSCs showed an anticipated negative correlation for the same gene set (NES: −2.98). Interestingly, analysis of a set of 50 upregulated genes in MPPs (from 65 genes that were significantly changed and correlated with the CFUe down signature),

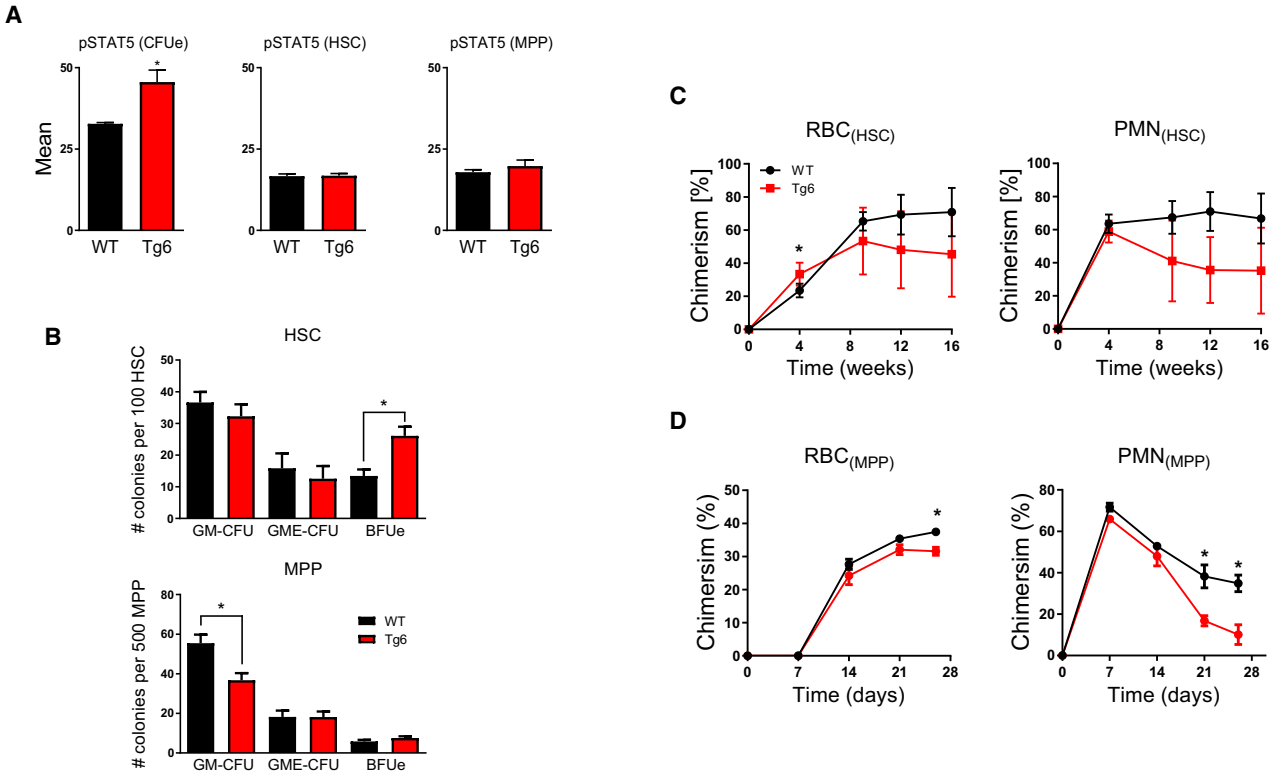

Figure 6. Differential Tg6 HSCs Display a Clear Erythroid Signature, while the MPP Fraction Has Two Opposing Signatures

(A) Mass cytometry to quantify the phosphorylated forms of STAT5 in freshly isolated CFUe's, HSCs, and MPPs from WT and Tg6 mice (n = 3–5).

(B) Bar graphs representing the number of colonies in the semi-solid *ex vivo* assay using HSCs or MPPs from both genotypes (n = 8).

(C and D) Transplantation assay in irradiated WT mice as depicted in Figure S5F. All mice were bled at the time points shown in (C) and (D) and peripheral blood chimerism was defined by FACS (n = 4–5). Data are representative for two to three independent experiments. All values are mean ± SEM. *p < 0.05.

See also Figure S5.

showed a highly significant association with monocytes, while the majority of the downregulated genes correlated with B lymphocytes (Enrichr/Jensen TISSUES analysis; Figure 5B) (Kuleshov et al., 2016; Lachmann et al., 2010). Further, we compared significantly modulated Tg6 transcripts with a set of Pre-GM genes, but were able to confirm a highly significant and positive correlation with only Tg6 MPPs (Figure 5A). Together, these analyses clearly reveal that Tg6 HSCs display an exclusive erythroid signature, whereas the Tg6 MPP population exhibited erythroid as well as myeloid signatures.

As our RNA-seq data revealed a significant 2-fold induction of *Epo-R* mRNA in Tg6 HSCs, we sought to assess the *in vivo* activation of the JAK/STAT and the MAPK-ERK1/2 pathways in both HSCs and MPPs using mass cytometry (Cytof). As expected, Tg6 CFUe cells showed significantly more phosphorylation of STAT5 compared with WT cells (Figure 6A); however, EPO/EPO-R pathways were not differentially activated in Tg6 HSCs, MPPs, or Pre-MgE cells (Figures 6A, S5A, and S5B). Subsequently, we performed a semi-solid colony-forming assay (no added EPO) using sorted HSCs and MPPs from both Tg6 and WT mice to understand the presence and extent of fate changes. In concurrence with our *in vivo* and deep-sequencing data, Tg6 HSCs yielded significantly higher erythroid progenitors (BFUe), while Tg6 MPPs exhibited a lower differentiation potential toward granulocyte/monocyte precursors (GM-CFU) (Figure 6B). In addition, we also defined the differentiation potential of MPP2 ($CD48^+/CD150^+$ LSK cells), positioned between HSC and MPP, with clear erythroid potential (Pietras et al., 2015). We reveal significantly more MPP2 in the BM of Tg6 mice, although without increase in cell-cycle progression (Figures S5C and S5D). Moreover, and in clear contrast to HSC or MPP, MPP2 showed no change in their differentiation potential to any of the observed progenitors (Figure S5E). These findings primarily show that the enhanced differentiation of Tg6 HSC to BFUe is independent of direct EPO signaling, and suggest that Tg6 HSCs

do not necessarily have to differentiate into MPPs (e.g., MPP2 or 3) to become erythroid progenitors. Furthermore, we examined the *in vivo* repopulation capacity of Tg6 HSCs and MPPs (Figure S5F), and demonstrated that Tg6 HSCs were able to produce significantly higher fractions of RBCs compared with WT HSCs at 4 weeks after transplantation, and that chimerism in RBCs and polymorphonuclear (PMN) cells was not significantly different between the two donor groups at 16 weeks (Figure 6C). Tg6 MPPs, on the other hand, lost their PMN differentiation potential more rapidly than WT MPPs (Figure 6D), confirming our initial findings (Figures 2C and 6B). Taken together, these results strongly suggest that chronic exposure to excessive EPO leads to differential fate changes in HSCs and MPPs.

DISCUSSION

In the current study, we used the EPO transgenic mouse line Tg6 and a combination of *in vivo, in vitro*, and deep-sequencing approaches to study the effects of chronic EPO stress on HSCs and their closest progenitors, the MPPs. We show that HSCs and MPPs display a clear differential response to such sustained stress. HSCs exhibit a committed erythroid progenitor profile with enhanced cell division and differentiation activity, while MPPs display opposing cell signatures and an accumulation of uncommitted cells.

Acute but short exposure of HSCs/MPPs to high EPO levels has been shown to result in the creation of an "erythroid superhighway" that generates erythroid progenitors via the classical intermediates (Grover et al., 2014); however, we show striking differences between HSC and MPP lineages in mice chronically exposed to high EPO. Essentially, while Tg6 HSCs showed enhanced proliferation with an induction of numerous cell-cycle-related genes, Tg6 MPPs remained more quiescent and displayed restrained differentiation. This highlights the differential response of both cell populations and strongly points to differentiation/proliferation of HSCs into erythroid progenitors in an environment of sustained exposure to high EPO. Further, although both Tg6 HSCs and MPPs showed a clear erythroid signature, only HSCs displayed a prominent increase in erythroid-related transcription factors and a 5-fold induction in *Klf1,* one of the genes with a GATA1-preferred site, which is regulated by it (Suzuki et al., 2013). Conversely, *Klf1* is even slightly downregulated in Tg6 MPPs (1.4-fold). Since this transcription factor was shown to stabilize GATA1's occupancy in the β-globin locus (Kang et al., 2015), it is conceivable that the stability of the GATA1 protein, but not *Gata1* mRNA, is reduced in Tg6 MPP, an effect that might eventually also be reflected in the overall increased expression of erythroid genes. KLF1 is also an important and tight regulator of erythroid lineage commitment that stimulates the expression of the EPO-R in erythroid progenitors, while inhibiting the thrombopoietin receptor (TPO-R or MPL [Shah et al., 2015]). Tg6 HSCs indeed display almost 2-fold higher *Epo-R* and lower *Mpl* expression, which resembles an erythroid-commitment model similar to megakaryocyte erythrocyte progenitors (Pre-MgE). Moreover, mass cytometry experiments revealed no differential activation of EPO/EPO-R signaling pathways in the HSC/MPP/Pre-MgE fractions of adult Tg6 mice versus WT littermates. Although one study has demonstrated a functional EPO-R on HSCs *in vitro* (Shiozawa et al., 2010), another report demonstrated no detectable EPO-R expression on non-erythroid hematopoietic progenitors using *in vivo* lineage tracing studies (Singbrant et al., 2011). Therefore, it is possible that specific but divergent fate changes in Tg6 HSCs and MPPs are indirectly induced by EPO-triggered erythroid progenitors or through stromal cells in the BM as suggested previously (Lodish et al., 2010). In this respect, we recently showed an effect of chronic EPO exposure on the bone niche, as Tg6 mice revealed significant reduction of bone volume related to diminished osteoblast and increased osteoclast activity (Hiram-Bab et al., 2015; Rauner et al., 2016). Endothelial cells are also BM niche cells containing a functional EPO-R (Trincavelli et al., 2013). Previously, it was shown that AKT1-activated BM endothelial cells display a distinct transcription factor and cytokine profile that can support functional HSCs under severe stress conditions (Poulos et al., 2015). Furthermore, in the colony assays using methylcellulose-containing medium without additional EPO, Tg6 HSCs preferentially differentiate into BFUe progenitors. The same cells also produce more erythrocytes up to 4 weeks after transplantation into WT mice. These results show that even preceding chronic exposure to high EPO leads to erythroid fate decision in HSCs, suggesting EPO-induced epigenetic changes. Further research is therefore required to unravel the (in)direct and/or temporal role of EPO/EPO-R on the bone/BM.

Although acute exposure to EPO decreases the Pre-GM signature in the HSC/MPP compartment (Grover et al., 2014), our comprehensive GSEA data analysis clearly linked Tg6 MPPs, but not HSCs, to the myeloid network, implying the existence of two clearly distinct signatures that apparently limited the contribution of MPPs to the response to the enhanced RBC demand. Despite the definitive innate immune signature, our observations from colony assays and Tg6 MPP transplantation experiments clearly show hampered differentiation into more mature myeloid progenitors. In addition, $CSF1R^{+}$-Tg6 MPPs expressed significantly less GATA1, indicating the existence of distinct erythroid and myeloid Tg6 MPP fractions.

To conclude, we show that EPO can induce transcriptional rewiring, which leads to continuous and chronic overproduction of erythroid progenitors largely driven by HSCs rather than MPPs. Moreover, our data show that a stepwise progression through specific differentiation stages is probably not essential for HSC lineage commitment, as also suggested previously (Yamamoto et al., 2013). Tg6 MPPs display two cell signatures with different functionalities that also result in hampered myeloid progenitor differentiation and the absence of erythroid progenitor overproduction. Our findings not only provide insights into the role of HSCs during erythroid stress, but may also have implications for other hematopoietic-related chronic disorders and long-term clinical therapies, including the application of EPO-stimulating agents.

EXPERIMENTAL PROCEDURES

Mice

All transgenic mice (Vogel and Gassmann, 2011) and their WT littermates were bred and maintained in our animal facility with *ad libitum* water and food. C57BL/6 (B6), B6.SJL-PtprcaPep3b/BoyJ (B6.SJL), and Ubc:GFP mice were purchased from the Jackson Laboratory. Experiments were performed with male and female mice (aged 3–5 months), and experimental procedures were approved by the local ethics committee.

Flow Cytometry and Sorting

Flow cytometry, cell sorting, and cell-cycle analyses were performed as described previously (Singh et al., 2013).

Transplantation

HSCs or MPPs were isolated from Ubc:GFP-Tg6 and Ubc:GFP WT littermates. A total of 5,000 Lin^- $cKIT^+$ $SCA\text{-}1^+$ $CD48^+$ $CD150^-$ (MPP) from WT-Ubc:GFP and littermate Tg6-Ubc:GFP or 300 $cKIT^+$ $SCA\text{-}1^+$ $CD48^-$ $CD150^+$ $CD34^-$ (HSC) were competitively transplanted together with non-fractionated 5×10^5 B6.SJL (CD45.1) BM cells into lethally irradiated (9 Gy) congenic WT recipients. Peripheral blood was analyzed on a BD fluorescence-activated cell sorting Canto or on a Sysmex.

Telomere Lengths

Sorted 5×10^4 MPPs were fixed with 70% Formamid, stained with PNA Cy3 probe and incubated for 10 min at 82°C. Consequent incubation overnight at room temperature (RT) after which samples were washed twice with 70% Formamid. DAPI solution was used to discriminate between G0/G1 and S/G2/M phases of the cell cycle. Samples were analyzed on LSRII and MFI for cells in G0/G1 phases was estimated.

Differential Gene Expression Analysis

Complete cDNA (pre-amplified for all HSC samples) was synthesized with the SMARTer Ultra HV Kit (Clontech). After ultrasonic shearing of the amplified cDNA (Covaris S2) samples were subjected to standard Illumina fragment library preparation using the NEBNext chemistries (New England Biolabs). Libraries were equimolarly pooled and sequenced on an Illumina HiSeq 2500, resulting in ca. 32–43 million single-end reads per library. After sequencing, FastQC (http://www.bioinformatics.babraham.ac.uk/) was used to perform a basic quality control on the sequencing data. As an additional control, library diversity was assessed by redundancy investigation in the reads. Next, the reads were aligned with BWA (v.0.7.8) against the mouse reference (mm10) and an exon-exon junction library of 120 nucleotides, which was created according to the Ensembl annotation version 69. The uniquely aligned reads were counted with featureCounts (v.1.4.4) and the same Ensembl annotation. Normalization of the raw read counts based on the library size and testing for differential expression between the two conditions was performed with the DESeq2 (v.1.4.0) R package. Genes with an adjusted p value of less than 0.1 were considered as differentially expressed for comparison. Differential gene expression analysis was performed using the DEseq2 R package to compare gene expression levels between Tg6 and WT mice for both HSC and MPP cell types. DEseq gave 6,629 significantly DEGs when comparing Tg and WT mice for HSC cells and 3,801 DEGs for MPP cells (p-adjusted value < 0.1). To compare DEGs between cell types we performed a simple overlap analysis (using Ensembl Gene IDs) to identify common and unique DEG, and performed a more fine-grained comparison by splitting DEGs into up and downregulated genes for each cell type.

GO Enrichment Analysis

Significantly differentially upregulated genes (p-adjusted value < 0.1, fold-change $\geq$ 2) from both HSCs and MPPs (710 genes HSC, 248 genes MPP) were mapped to Entrez Gene and analyzed using the clusterProfiler R package for GO term enrichment (enrichGO function, GO:BP ontology, p value cut-off = 0.1, BH adjusted p value cutoff 0.00001 (Yu et al., 2012). A selection of the GO terms represented in Figures 3B and 4A, include genes as shown in (Tables S1 and S2).

Gene Set Enrichment Analysis

Gene set enrichment analysis (GSEA) was used to compare gene lists from other cell types, namely Pre-MgE, MkP, Pre-GM, CLP (Sanjuan-Pla et al., 2013), CFUe up- and downregulated genes from (Li et al., 2014). GSEA analysis was performed using GSEA software from the Broad Institute (Mootha et al., 2003; Subramanian et al., 2005). HSC and MPP were ranked by log2 fold-change, the two lists were imported, lists pre-ranked, and compared against gene lists from cell types stated above.

Overlap Analysis

Comparisons between Pre-GM and DEGs from HSCs and MPPs were performed (overlap diagram based on gene symbols) along with a similar comparison for CFUe Down, HSC, and MPP DEGs. Genes unique to Pre-GM and MPP gene lists were then input into the Cytoscape plugin CLUEGO for further characterization, and identical analysis was also performed on genes unique to CFUe Down and MPP sets. Plots to compare log2 fold-change for genes unique to Pre-GM and HSC, and Pre-GM and MPP were created, along with a similar analysis for CFUe Down genes.

Mass Cytometry

BM cells from two femurs and two tibia were used for mass cytometry obtained by crushing in PBS and immediately fixed with Maxpar Fix I Buffer (Fluidigm) for 30 min at room temperature. For surface staining, cells were incubated with antibodies labeled with Metal-tags (CD150-167ER [cat. no. 3167004B], CD48-156Gd [cat. no. 3156012B], CD117-173Yb [cat. no. 3143001B], SCA-1 169Tm [cat. no. 3169015B], CD41-143Nd [cat. no. 3143009B]; [Fluidigm] and CD105PE [cat. no. 12-1051-82]; [eBioscience], and for the secondary step anti-phycoerythrin [MaxPar Ready] labeled with 160Gd [cat. no. 408105]; [Biolegend]). Next, cells were fixed and stained with specific metal tags antibodies against phosphorylated proteins (pAKT (S473)-152Sm [cat. no. 3152005A], pSTAT5 (Y694) [cat. no. 3150005A], pERK1/2 (T202/Y204)-171Yb [cat. no. 3171010A]; [Fluidigm]). Cells were incubated overnight in MaxPar Fix and Perm Buffer (Fluidigm) with 1:10,000 dilution Cell-ID Intercalator-Ir (Fluidigm), and analyzed on CyTOF2.

Immunocytochemistry

Different cell populations were sorted directly on to slides, dried at RT, fixed, incubated with GATA1 Alexa Fluor 647 antibody (cat. no. sc-265 AF647) (Santa Cruz Biotechnology), and analyzed on a Leica TCS SP5 confocal microscope.

Semi-solid Colony-Forming Assay

One hundred HSCs and 500 MPPs were sorted and cultivated in duplicate in methylcellulose-containing medium (MethoCult M3434). Colonies were counted microscopically at day 7.

Statistics

Data are presented as mean ± SEM. Significance was calculated using the Mann-Whitney U test. All statistical analysis was performed using GraphPad Prism v.6.03 (GraphPad, La Jolla, CA). Significance was set at $p < 0.05$. n in the figure legends always denotes individual mice.

ACCESSION NUMBERS

The RNA-seq data have been deposited in the Gene Expression Omnibus database (GEO: GSE113053).

SUPPLEMENTAL INFORMATION

Supplemental Information includes five figures and two tables and can be found with this article online at https://doi.org/10.1016/j.stemcr.2018.04.012.

AUTHOR CONTRIBUTIONS

R.P.S. and T.G. designed the study, performed the experiments, analyzed the data, and contributed toward writing the manuscript. B.R., M.M., and K.F. designed and performed the experiments. M.L. and A.D. performed the deep sequencing analyses. I.M., M.G., and T.C. provided tools and contributed to the discussions and writing the manuscript. I.H. performed the bioinformatics analyses, provided the tools, and contributed to the discussions and writing the manuscript. B.W. designed the study, supervised the overall project, analyzed the data, and wrote the manuscript.

ACKNOWLEDGMENTS

We would like to thank Anja Krüger and Antje Muschter for excellent technical assistance, Dr. Vasuprada Iyengar for critically reading the manuscript, and Claudia Waskow for sharing Tg6 mice. R.P.S., T.G., B.R., K.F., and B.W. were supported by the Emmy Noether and Heisenberg program (Deutsche Forschungsgemeinschaft–DFG, Germany) and M.G. by the Swiss National Science Foundation. This work was supported by the European Community's Seventh Framework Program under grant agreement no. 602699 (to T.C.), by the ERC (to T.C.), by grants from Deutsche Forschungsgemeinschaft (SFB655 Project B10 and SFB-TR127 Project A3 to T.C., GR4857/1-1 to T.G., and WI3291/1-1, 1–2 and 5-1 to B.W.), by a CRTD seed grant to T.G. and B.W., and by a GIF grant (no. I-1433-203.13/2017) to B.W. T.G. received support from the Fritz Thyssen Foundation (10.14.2.153) and K.F. from the "Maria Reiche program" from the Medical Faculty of the TU Dresden.

Received: November 8, 2017
Revised: April 13, 2018
Accepted: April 16, 2018
Published: May 10, 2018

REFERENCES

Akashi, K., Traver, D., Miyamoto, T., and Weissman, I.L. (2000). A clonogenic common myeloid progenitor that gives rise to all myeloid lineages. Nature *404*, 193–197.

Baldridge, M.T., King, K.Y., Boles, N.C., Weksberg, D.C., and Goodell, M.A. (2010). Quiescent haematopoietic stem cells are activated by IFN-gamma in response to chronic infection. Nature *465*, 793–797.

Bresnick, E.H., Lee, H.Y., Fujiwara, T., Johnson, K.D., and Keles, S. (2010). GATA switches as developmental drivers. J. Biol. Chem. *285*, 31087–31093.

Busch, K., Klapproth, K., Barile, M., Flossdorf, M., Holland-Letz, T., Schlenner, S.M., Reth, M., Hofer, T., and Rodewald, H.R. (2015). Fundamental properties of unperturbed haematopoiesis from stem cells in vivo. Nature *518*, 542–546.

Chiu, C.P., Dragowska, W., Kim, N.W., Vaziri, H., Yui, J., Thomas, T.E., Harley, C.B., and Lansdorp, P.M. (1996). Differential expression of telomerase activity in hematopoietic progenitors from adult human bone marrow. Stem Cells *14*, 239–248.

Clapes, T., Lefkopoulos, S., and Trompouki, E. (2016). Stress and non-stress roles of inflammatory signals during HSC emergence and maintenance. Front. Immunol. *7*, 487.

Dumitriu, B., Bhattaram, P., Dy, P., Huang, Y., Quayum, N., Jensen, J., and Lefebvre, V. (2010). Sox6 is necessary for efficient erythropoiesis in adult mice under physiological and anemia-induced stress conditions. PLoS One *5*, e12088.

Dunlop, E.A., Percy, M.J., Boland, M.P., Maxwell, A.P., and Lappin, T.R. (2006). Induction of signalling in non-erythroid cells by pharmacological levels of erythropoietin. Neurodegener. Dis. *3*, 94–100.

Franke, K., Gassmann, M., and Wielockx, B. (2013a). Erythrocytosis: the HIF pathway in control. Blood *122*, 1122–1128.

Franke, K., Kalucka, J., Mamlouk, S., Singh, R.P., Muschter, A., Weidemann, A., Iyengar, V., Jahn, S., Wieczorek, K., Geiger, K., et al. (2013b). HIF-1alpha is a protective factor in conditional PHD2-deficient mice suffering from severe HIF-2alpha-induced excessive erythropoiesis. Blood *121*, 1436–1445.

Gassmann, M., and Muckenthaler, M.U. (2015). Adaptation of iron requirement to hypoxic conditions at high altitude. J. Appl. Physiol. (1985) *119*, 1432–1440.

Grover, A., Mancini, E., Moore, S., Mead, A.J., Atkinson, D., Rasmussen, K.D., O'Carroll, D., Jacobsen, S.E., and Nerlov, C. (2014). Erythropoietin guides multipotent hematopoietic progenitor cells toward an erythroid fate. J. Exp. Med. *211*, 181–188.

Gutierrez, L., Tsukamoto, S., Suzuki, M., Yamamoto-Mukai, H., Yamamoto, M., Philipsen, S., and Ohneda, K. (2008). Ablation of Gata1 in adult mice results in aplastic crisis, revealing its essential role in steady-state and stress erythropoiesis. Blood *111*, 4375–4385.

Haas, S., Hansson, J., Klimmeck, D., Loeffler, D., Velten, L., Uckelmann, H., Wurzer, S., Prendergast, A.M., Schnell, A., Hexel, K., et al. (2015). Inflammation-induced emergency megakaryopoiesis driven by hematopoietic stem cell-like megakaryocyte progenitors. Cell Stem Cell *17*, 422–434.

Harandi, O.F., Hedge, S., Wu, D.C., McKeone, D., and Paulson, R.F. (2010). Murine erythroid short-term radioprotection requires a BMP4-dependent, self-renewing population of stress erythroid progenitors. J. Clin. Invest. *120*, 4507–4519.

Hiram-Bab, S., Liron, T., Deshet-Unger, N., Mittelman, M., Gassmann, M., Rauner, M., Franke, K., Wielockx, B., Neumann, D., and Gabet, Y. (2015). Erythropoietin directly stimulates osteoclast precursors and induces bone loss. FASEB J. *29*, 1890–1900.

Huang da, W., Sherman, B.T., and Lempicki, R.A. (2009). Systematic and integrative analysis of large gene lists using DAVID bioinformatics resources. Nat. Protoc. *4*, 44–57.

Humbert, P.O., Rogers, C., Ganiatsas, S., Landsberg, R.L., Trimarchi, J.M., Dandapani, S., Brugnara, C., Erdman, S., Schrenzel, M., Bronson, R.T., et al. (2000). E2F4 is essential for normal erythrocyte maturation and neonatal viability. Mol. Cell *6*, 281–291.

Kang, Y., Kim, Y.W., Yun, J., Shin, J., and Kim, A. (2015). KLF1 stabilizes GATA-1 and TAL1 occupancy in the human beta-globin locus. Biochim. Biophys. Acta *1849*, 282–289.

Kuleshov, M.V., Jones, M.R., Rouillard, A.D., Fernandez, N.F., Duan, Q., Wang, Z., Koplev, S., Jenkins, S.L., Jagodnik, K.M., Lachmann, A., et al. (2016). Enrichr: a comprehensive gene set enrichment analysis web server 2016 update. Nucleic Acids Res. *44*, W90–W97.

Lachmann, A., Xu, H., Krishnan, J., Berger, S.I., Mazloom, A.R., and Ma'ayan, A. (2010). ChEA: transcription factor regulation inferred from integrating genome-wide ChIP-X experiments. Bioinformatics *26*, 2438–2444.

Li, J., Hale, J., Bhagia, P., Xue, F., Chen, L., Jaffray, J., Yan, H., Lane, J., Gallagher, P.G., Mohandas, N., et al. (2014). Isolation and transcriptome analyses of human erythroid progenitors: BFU-E and CFU-E. Blood *124*, 3636–3645.

Lodish, H., Flygare, J., and Chou, S. (2010). From stem cell to erythroblast: regulation of red cell production at multiple levels by multiple hormones. IUBMB Life *62*, 492–496.

Mootha, V.K., Lindgren, C.M., Eriksson, K.F., Subramanian, A., Sihag, S., Lehar, J., Puigserver, P., Carlsson, E., Ridderstrale, M., Laurila, E., et al. (2003). PGC-1alpha-responsive genes involved in oxidative phosphorylation are coordinately downregulated in human diabetes. Nat. Genet. *34*, 267–273.

Nilsson, R., Schultz, I.J., Pierce, E.L., Soltis, K.A., Naranuntarat, A., Ward, D.M., Baughman, J.M., Paradkar, P.N., Kingsley, P.D., Culotta, V.C., et al. (2009). Discovery of genes essential for heme biosynthesis through large-scale gene expression analysis. Cell Metab. *10*, 119–130.

Pietras, E.M., Mirantes-Barbeito, C., Fong, S., Loeffler, D., Kovtonyuk, L.V., Zhang, S., Lakshminarasimhan, R., Chin, C.P., Techner, J.M., Will, B., et al. (2016). Chronic interleukin-1 exposure drives haematopoietic stem cells towards precocious myeloid differentiation at the expense of self-renewal. Nat. Cell Biol. *18*, 607–618.

Pietras, E.M., Reynaud, D., Kang, Y.A., Carlin, D., Calero-Nieto, F.J., Leavitt, A.D., Stuart, J.M., Gottgens, B., and Passegue, E. (2015). Functionally distinct subsets of lineage-biased multipotent progenitors control blood production in normal and regenerative conditions. Cell Stem Cell *17*, 35–46.

Poulos, M.G., Crowley, M.J., Gutkin, M.C., Ramalingam, P., Schachterle, W., Thomas, J.L., Elemento, O., and Butler, J.M. (2015). Vascular platform to define hematopoietic stem cell factors and enhance regenerative hematopoiesis. Stem Cell Reports *5*, 881–894.

Pronk, C.J., Rossi, D.J., Mansson, R., Attema, J.L., Norddahl, G.L., Chan, C.K., Sigvardsson, M., Weissman, I.L., and Bryder, D. (2007). Elucidation of the phenotypic, functional, and molecular topography of a myeloerythroid progenitor cell hierarchy. Cell Stem Cell *1*, 428–442.

Rauner, M., Franke, K., Murray, M., Singh, R.P., Hiram-Bab, S., Platzbecker, U., Gassmann, M., Socolovsky, M., Neumann, D., Gabet, Y., et al. (2016). Increased EPO levels are associated with bone loss in mice lacking PHD2 in EPO-producing cells. J. Bone Miner. Res. *31*, 1877–1887.

Ruschitzka, F.T., Wenger, R.H., Stallmach, T., Quaschning, T., de Wit, C., Wagner, K., Labugger, R., Kelm, M., Noll, G., Rulicke, T., et al. (2000). Nitric oxide prevents cardiovascular disease and determines survival in polyglobulic mice overexpressing erythropoietin. Proc. Natl. Acad. Sci. USA *97*, 11609–11613.

Sanjuan-Pla, A., Macaulay, I.C., Jensen, C.T., Woll, P.S., Luis, T.C., Mead, A., Moore, S., Carella, C., Matsuoka, S., Bouriez Jones, T., et al. (2013). Platelet-biased stem cells reside at the apex of the haematopoietic stem-cell hierarchy. Nature *502*, 232–236.

Sawai, C.M., Babovic, S., Upadhaya, S., Knapp, D., Lavin, Y., Lau, C.M., Goloborodko, A., Feng, J., Fujisaki, J., Ding, L., et al. (2016). Hematopoietic stem cells are the major source of multilineage hematopoiesis in adult animals. Immunity *45*, 597–609.

Seita, J., Sahoo, D., Rossi, D.J., Bhattacharya, D., Serwold, T., Inlay, M.A., Ehrlich, L.I., Fathman, J.W., Dill, D.L., and Weissman, I.L. (2012). Gene Expression Commons: an open platform for absolute gene expression profiling. PLoS One *7*, e40321.

Shah, N.A., Levesque, M.J., Raj, A., and Sarkar, C.A. (2015). Robust hematopoietic progenitor cell commitment in the presence of a conflicting cue. J. Cell Sci. *128*, 4024.

Shiozawa, Y., Jung, Y., Ziegler, A.M., Pedersen, E.A., Wang, J., Wang, Z., Song, J., Wang, J., Lee, C.H., Sud, S., et al. (2010). Erythropoietin couples hematopoiesis with bone formation. PLoS One *5*, e10853.

Singbrant, S., Russell, M.R., Jovic, T., Liddicoat, B., Izon, D.J., Purton, L.E., Sims, N.A., Martin, T.J., Sankaran, V.G., and Walkley, C.R. (2011). Erythropoietin couples erythropoiesis, B-lymphopoiesis, and bone homeostasis within the bone marrow microenvironment. Blood *117*, 5631–5642.

Singh, R.P., Franke, K., Kalucka, J., Mamlouk, S., Muschter, A., Gembarska, A., Grinenko, T., Willam, C., Naumann, R., Anastassiadis, K., et al. (2013). HIF prolyl hydroxylase 2 (PHD2) is a critical regulator of hematopoietic stem cell maintenance during steady-state and stress. Blood *121*, 5158–5166.

Stanley, E.R., and Chitu, V. (2014). CSF-1 receptor signaling in myeloid cells. Cold Spring Harb. Perspect. Biol. *6*. 10.1101/cshperspect.a021857.

Subramanian, A., Tamayo, P., Mootha, V.K., Mukherjee, S., Ebert, B.L., Gillette, M.A., Paulovich, A., Pomeroy, S.L., Golub, T.R., Lander, E.S., et al. (2005). Gene set enrichment analysis: a knowledge-based approach for interpreting genome-wide expression profiles. Proc. Natl. Acad. Sci. USA *102*, 15545–15550.

Sun, J., Ramos, A., Chapman, B., Johnnidis, J.B., Le, L., Ho, Y.J., Klein, A., Hofmann, O., and Camargo, F.D. (2014). Clonal dynamics of native haematopoiesis. Nature *514*, 322–327.

Suzuki, M., Kobayashi-Osaki, M., Tsutsumi, S., Pan, X., Ohmori, S., Takai, J., Moriguchi, T., Ohneda, O., Ohneda, K., Shimizu, R., et al. (2013). GATA factor switching from GATA2 to GATA1 contributes to erythroid differentiation. Genes Cells *18*, 921–933.

Trincavelli, M.L., Da Pozzo, E., Ciampi, O., Cuboni, S., Daniele, S., Abbracchio, M.P., and Martini, C. (2013). Regulation of erythropoietin receptor activity in endothelial cells by different erythropoietin (EPO) derivatives: an in vitro study. Int. J. Mol. Sci. *14*, 2258–2281.

Trumpp, A., Essers, M., and Wilson, A. (2010). Awakening dormant haematopoietic stem cells. Nat. Rev. Immunol. *10*, 201–209.

Vogel, J., and Gassmann, M. (2011). Erythropoietic and non-erythropoietic functions of erythropoietin in mouse models. J. Physiol. *589*, 1259–1264.

Wilson, A., Laurenti, E., Oser, G., van der Wath, R.C., Blanco-Bose, W., Jaworski, M., Offner, S., Dunant, C.F., Eshkind, L., Bockamp, E., et al. (2008). Hematopoietic stem cells reversibly switch from dormancy to self-renewal during homeostasis and repair. Cell *135*, 1118–1129.

Yamamoto, R., Morita, Y., Ooehara, J., Hamanaka, S., Onodera, M., Rudolph, K.L., Ema, H., and Nakauchi, H. (2013). Clonal analysis unveils self-renewing lineage-restricted progenitors generated directly from hematopoietic stem cells. Cell *154*, 1112–1126.

Yu, G., Wang, L.G., Han, Y., and He, Q.Y. (2012). clusterProfiler: an R package for comparing biological themes among gene clusters. OMICS *16*, 284–287.